Indian Journal of Chemistry
Vol. 58B, February 2019, pp. 200-208

Solvent directed self-assembly of naphthalenediimide-tryptophan-glutamate conjugates

Santosh P Goskulwad[a], Vishal G. More[b], Duong Duc La[c], Rajesh S Bhosale[a], Avinash L Puyad[d]
Sidhanath V Bhosale[a] & Sheshanath V Bhosale*[b]

[a] Polymers and Functional Materials Division and Academy of Scientific and Innovative Research (AcSIR), CSIR-Indian Institute of Chemical Technology, Hyderabad 500 007, India
[b] Department of Chemistry, Goa University, Taleigao Plateau, Goa 403 206, India
[c] Institute of Chemistry and Materials, 17 Hoang Sam, Cay Giay, Hanoi, Vietnam
[d] School of Chemical Sciences, Swami Ramanand Teerth Marathwada University, Nanded 431 606, India
E-mail: bhosale@iict.res.in; svbhosale@unigoa.ac.in

Received 13 July 2018

We have designed and synthesised NDI derivatives bearing L-Trp-L-Glu methyl ester (**Trp-GLU**) and studied their self-assembly in THF-MCH and THF-H_2O solvent mixes. The optical properties of **NDI-Trp-GLU** in solution have been investigated by means of UV-Vis absorption and fluorescence spectroscopic techniques and redox properties have been examined using cyclic voltammogram. Interestingly, **NDI-Trp-GLU** self-assembled into microflowers and microfibers with increasing proportion of MCH and H_2O solvent, respectively, which suggests that solvophobic control is important for self-assembly phenomenon.

Keywords: Supramolecular self-assembly, naphthalene diimide, glutamate, tryptophan, superstructures

Non-covalent interactions such as hydrogen-bonding, electrostatic, van der Waals, hydrophobic and π-π intercations are involved in supramolecular self-assembly and self-organisation of small organic molecules and have been extensively studied in recent years[1]. Fabrication of functional nanodevices from small organic molecules and its applications to mimic biological systems requires detail mechanistic approach[2]. This helps to investigate the self-assembly process and the obtained nanostructures of such self-organised systems. To fabricate such tailor-made functional architectures naphthalene diimides (NDIs) are an ideal π-conjugated building blocks[3], due to their potential n-type semiconducting properties and also potential applications in organic photovoltaics (OPV), dye sensitised solar cells (DSSC), organic light emitting diodes (OLED) and organic field effect transistors (OFETS)[4]. Due to the formation of molecular assembly through non-covalent intercations, especially π-π stacking, use of NDI became very prominent in supramolecular chemistry. In the last two decades, several groups used NDI and their derivatives for formation of molecular self-assemblies with various nanoarchitectures, such as nanowires, nanoparticles, nanoflowers, nanobelts and nanofibers like nanostuctures[3,5]. During fabrication of such self-assembled materials there are clear indication that small change in environment such as solvent, temperature, *p*H and analytes or minor alteration in the structures can tune the self-assembled nanostructures[6].

Use of amino acids and peptides along with optically active dyes have been used to fabricate supramolecular self-assembled functional nanostructures[7]. Recently, Sarkar *et al.* showed tryptophan (Trp) alone to form self-assembled nanotubes[8]. Stoikov and co-workers reported *p*-tert-butylthiacalix[4]arene-L-tryptophan conjugate self-assembled into chiral fluorescent nanoparticles[9]. Saha *et al.* investigated the self-assembled nanostructure formation of tryptophan derivative containing long alkyl chain[10]. Liu *et al.* studied synthesis and self-assembly of L-glutamic acid based bolaamphiphile, which yields helical spherical-nanotubes[11]. Furthermore, the self-assembly of different types of NDI-amino acid and NDI-peptide derivatives in various solvent systems have been also reported[12,13]. Recently, we reported synthesis and self-assembly of NDI-peptide amphiphile into golf-ball like morphology[14] as well as the formation of nanofibers

and flower-like nanostructures[15]. Though the field is rapidly developing there is still a need to investigate design and self-assembly of NDI-peptide based system due to their utility in various fields. Based on above factors, we presume that the combination of L-glutamic acid ester and polar aromatic amino acid such as tryptophan with optically active NDI dye may lead to newer supramolecular structures. These results prompted us to design the novel NDI-peptide conjugate based on L-glutamic acid ester and aromatic amino acid, particularly L-tryptophan.

In continuation of our work to understand the effect of aromatic ring system on self-assembly of naphthalenediimide, we designed and synthesised NDI-Trp-Glu conjugate (Scheme I) and investigated its self-assembly in various solvents. The self-assembly formation were studied in varing proportion of MCH and water-THF solvent system, respectively. The designed molecule having three important features for supramolecular self-assembly and self-organisation: 1) aromatic NDI core provide π-π interactions 2) NDI bearing peptide headgroup is responsible for hydrogen bonding along with van der Waals interactions and 3) the effect of indole ring subunit present in the tryptophan. These properties are responsible for the formation of microsheet self-assembled morphologies and fiber formation in THF:MCH at 40:60 vol% and 20:80 vol% solvent compositions, respectively. Scanning electron microscopy (SEM) imaging demonstrates formation of puzzle like morphology and long fibril structures in THF:MCH at 40:60 vol% and 20:80 vol% solvent compositions, respectively. Whereas, in THF:H_2O at 40:60 vol% and 20:80 vol% solvent mixes **NDI-Trp-GLU** leads to formation of microflowers and microfibers, respectively.

Experimental Section

Materials, Instruments and Methods

All chemicals were purchased from Sigma-Aldrich Pvt. Ltd., Bengaluru, Karnataka, India. Solvents used for reactions were of reagent grade. Silica gel was used as stationary phase for column chromatography. The UV-Vis spectra were recorded using Shimadzu UV-Vis-1800 UV-Vis experiments were performed in 3 mL THF solution, quartz cuvette and recorded with incremental addition of MCH and water, respectively. The fluorescence emission measurements were recorded using Shimadzu RF-6000 instruments. Fluorescence emission experiments were operated in a quartz cell with a 1 cm path length upon excitation at 360 nm wavelength. The cyclic voltammetry data were recorded at RT on Autolab 302 N instrument. Cyclic voltammetry measurements were recorded at a concentration of 1×10^{-4}M in THF containing tetra-*n*-butyl ammonium hexafluoro-phosphate (Bu_4NPF_6 0.1M) as supporting electrolyte with a platinum working electrode and Calomel as a quasi-reference electrode. The $E_{1/2}$ values for the **NDI-Trp-GLU** were determined relative to the ferrocenium/ferrocene (Fc^+/Fc) redox couple as an internal standard. The reduction potentials calculated for **NDI-Trp-GLU** are relative to Fc^+/Fc couple value as 0.0 V. The Gaussian 09 *ab initio*/DFT quantum chemical simulation package was employed to get results of the calculations in the present work[17-19]. The geometry optimization of **NDI-Trp-GLU** molecule has been carried out at B3LYP/6-31G(d) level of theory. The DLS measurements were performed on Malvern Nano ZS instrument. The volume of the solution in cuvette was 3 mL and the final concentration of **NDI-Trp-GLU** was 1×10^{-4}M. Scanning electron microscopy images were recorded by solvent evaporation on a silicon wafer and then sputter coated with gold for 10 s at 0.016 mA Ar plasma (SPI, West Chester, USA). The SEM imaging was performed using a FEI Nova NanoSEM (Hillsboro, USA) operating at high vacuum at the voltage of 15 keV.

Synthesis of compound 1[16]

1,4,5,8-Naphthalene tetracarboxylic dianhydride (0.5 g, 1.8 mmol) and L-tryptophan (0.6g. 1.8 mmol) were suspended in 20 mL of dry DMF. To this

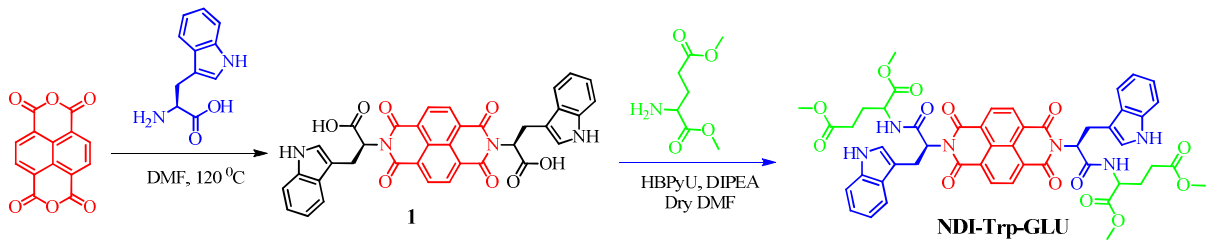

Scheme I — Synthesis of compound **NDI-Trp-GLU**

suspension Et_3N (0.2 mL) was added and the mixture allowed to reflux for 15 h. After cooling the reaction mixture to RT, the precipitate was filtered and recrystallized from ethanol to yield 700 mg (58%) of compound **1**. m.p.350-54°C. ^{1}H NMR (300 MHz, DMSO-d_6): δ 9.14 (2H, s), 8.52 (4H, s), 7.53-7.50 (2H, d), 7.20-7.17 (2H, d), 7.01-6.86 (6H, m), 6.04-5.99 (2H, m), 3.83-3.64 (4H, m); ^{13}C NMR ($CDCl_3$, 75 MHz): δ 169.3, 160.5, 134.6, 129.4, 125.6, 124.5, 121.7, 119.4, 116.4, 109.8, 108.7, 52.92, 34.71, 29 62, 22.80; ESI-MS: *m/z* $[M+H]^+$ 641; IR (KBr): 3367 (O-H), 2931 (C-H), 1703 (acidic C=O), 1665 cm^{-1} (NDI, C=O).

Synthesis of NDI-1(NDI-Trp-GLU)

In a 25 mL round bottomed flask compound **1** (100 mg, 0.15 mmol) and HBPyU (215 mg, 0.50 mmol) was added to a 15 mL dry DMF under nitrogen atmospheric condition. The reaction mixture was stirred for 30 min at 0°C. Glutamic dimethyl ester (113 mg, 0.45 mmol) and DIPEA (65 mg, 0.50mmol) were added to the reaction mixture. The resulting reaction mixture was stirred for 15 h at RT. After completion of the reaction (monitored by TLC) solvent was removed by rotary evaporator under reduced pressure. The reaction mixture was eluted with dichloromethane (50 mL) and washed with aqueous 10% w/v $NaHCO_3$ solution (2 × 30 mL), followed by water (20 mL) and brine (20 mL). The resultant organic layer was dried over anhydrous sodium sulphate, filtered and concentrated *in vacuo*. The residue was purified by silica gel column chromatography eluting with 4% methanol: dichloromethane solution to afford the desired product as brick red solid as **NDI-Trp-GLU** (95 mg, 64%). m.p.244-46°C. ^{1}H NMR (300 MHz, $CDCl_3$): δ 8.66 (4H, s), 7.75-7.74 (2H, d, *J* = 7.93 Hz), 7.68-7.63 (2H, d, *J* = 7.47 Hz), 7.29-7.27 (2H, m), 7.20 (2H, s), 7.15-7.14 (2H, t, *J* = 7.78 Hz), 7.11-7.09 (2H, t, *J* = 7.93), 6.29-6.26 (2H, t, *J* = 8.80 Hz), 4.73-4.69 (2H, q), 3.97-3.92 (2H, m), 3.82 (6H, s), 3.60-3.54 (2H, m), 3.56 (6H. s), 2.16-1.12 (4H, q), 2.11-2.07 (2H, q) 1.86-1.82 (2H, q); ^{13}C NMR ($CDCl_3$ 75 MHz): δ 174.84, 172.34, 171.59, 162.78, 159.61, 159.27, 136.38, 131.35, 126.21, 123.19, 122.89, 120.14, 118.61, 115.49, 113.22, 111.42, 54.48, 53.26, 52.44, 52.39, 29.47, 26.48, 25.21; IR (KBr): 3368 (N-H), 2925 (C-H), 1738 (Ester C=O), 1707 (amide C=O), 1669 cm^{-1} (NDI C=O); ESI-MS: *m/z* Calcd for $C_{50}H_{46}N_6O_{14}$: 954.93. Found: $[M+H]^+$ 956; ESI-HRMS: *m/z* Calcd for $C_{50}H_{47}N_6O_{14}$: 955.315. Found: 955.314.

Results and Discussion

Synthesis

The synthesis of NDI derivative **NDI-Trp-GLU** is shown in Scheme I, typically, **1** was synthesized by condensation reaction of commercial available 1,4,5,8-naphthalenetetracarboxylic dianhydride with tryptophan in DMF at 120°C for 24 h[16]. Furthermore, the molecule **1** was reacted with methyl ester of glutamic acid in presence of HBPyU in presence of DIPEA to yield compound **NDI-Trp-GLU**. The obtained derivative was fully characterised by using FT-IR, ^{1}H NMR, ^{13}C NMR, mass and HRMS techniques. The thermal stability of **NDI-Trp-GLU** was investigated by using thermo gravimetric analysis (TGA, Figure S1) and differential scanning calorimetry (DSC, Figure S2) techniques under nitrogen atmosphere. For NDI-Trp-GLUa decomposition temperature of 5% weight loss was observed at 246°C temperatures. Whereas DSC measurements showed crystalline temperature at 197.5°C and two melting point temperatures at 255°C and 269°C, suggesting the thermal stability of compound.

Cyclic Voltammetry

Cyclic voltammetry (CV) was employed to investigate the electrochemical properties of **NDI-Trp-GLU** (Figure 1). CV experiment of **NDI-Trp-GLU** was performed in 0.1 M Bu_4PF_6 in dichloromethane displayed reversible reduction wave with the reduction potential in between −0.44 to −0.66 V potential. The onset reduction potential is −0.55 V. We employed the formula $E_{LUMO} = -e\,[E_{red}^{onset} + 4.4]$ eV to calculate LUMO values of **NDI-Trp-GLU**.

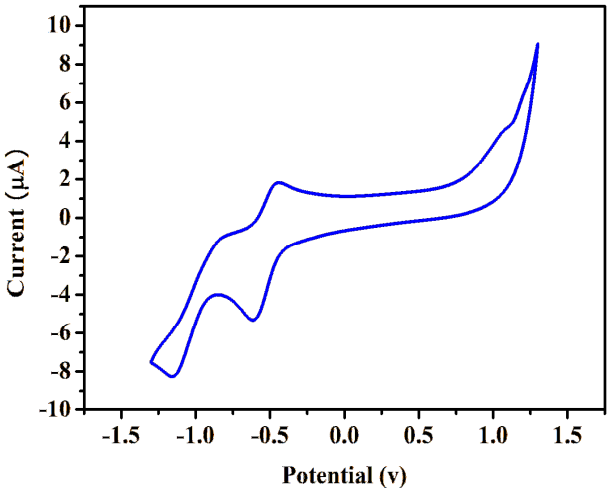

Figure 1 — Cyclic voltammetry of compound **NDI-Trp-GLU**(1×10^{-4} M) in THF containing Bu_4NPF_6 (0.1 M) electrolyte.

Using onset reduction potential, the calculated E_{LUMO} value is −3.85 eV, indicating **NDI-Trp-GLU** is good acceptor[4].

Furthermore, we have employed DFT calculations for **NDI-Trp-GLU** at the B3LYP/6-31G(d) level of theory[17]. The optimized structure of **NDI-Trp-GLU** along with HOMO and LUMO wave functions are generated by using Avogadro and are depicted in Figure 2[18,19]. HOMO resides mainly on tryptophan subunits whereas LUMO is localized over the NDI subunit. The calculated LUMO value for **NDI-Trp-GLU** is −3.25668 eV as shown in ESI Table S1a and 1b. These results clearly suggest that **NDI-Trp-GLU** act as an electron acceptor. The geometries of **NDI-Trp-GLU** obtained at B3LYP/6-31G(d) level were subjected to time-dependent density functional theory (TD-DFT) at the same level of theory and **NDI-Trp-GLU** shows absorption at 369 nm (Figure S3)

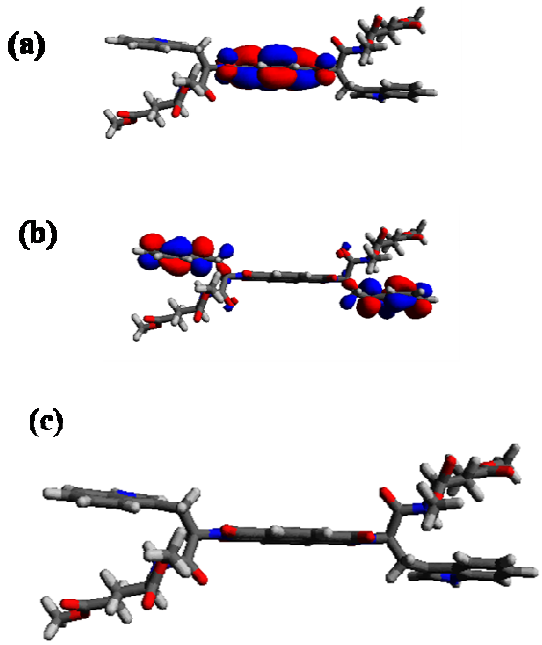

Figure 2 — B3LYP/6-31G(d) predicted (a) LUMO; (b) HOMO orbitals and (c) optimized structure of **NDI-Trp-GLU** compound.

UV-Vis absorption studies and Fluorescence emission studies

To examine mode of aggregation in solvent mixtures THF:MCH and THF:H_2O, we employed

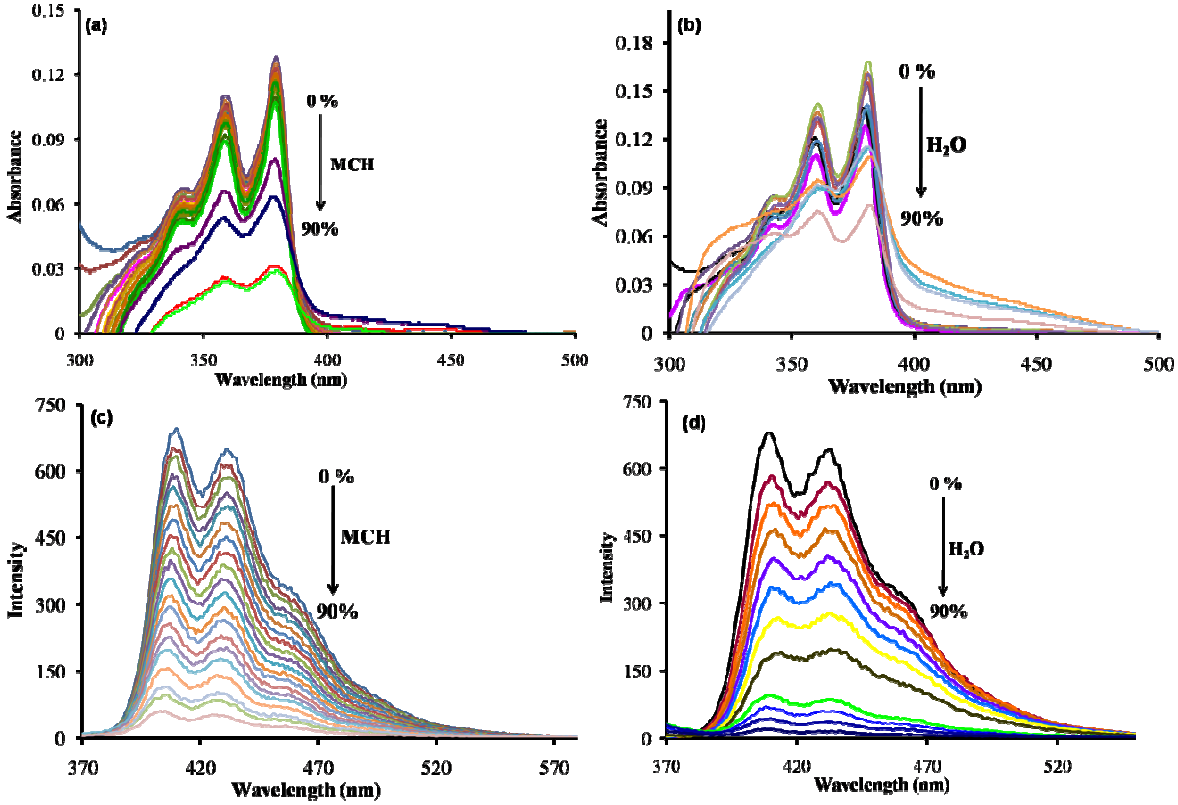

Figure 3 — UV-Vis absorption and emission spectra of **NDI-Trp-GLU** (1×10^{-5} M) in THF upon addition of (a & c) MCH; (b & d) H_2O, respectively.

UV-Vis absorption and fluorescence techniques. At first glance we performed UV-Vis absorption experiments of compound **NDI-Trp-GLU** in pure THF (1×10^{-5} M). NDI-Trp-GLU exhibits two major absorption peaks at 360 nm and 380 nm along with a shoulder peak at 342 nm (Figure 3a). The absorption peaks at 360 nm and 380 nm attributed to the π-π* transition of the NDI chromophore. A solvent dependent absorption spectroscopic MCH in THF solution, decrease in intensities of all the peaks was observed. At a THF:MCH, 10:90 composition the shoulder peak disappeared and the two peaks at 360 and 380 nm were significantly decreased. Moreover, UV-Vis absorption maxima of **NDI-Trp-GLU** at 380 nm were plotted against the % added MCH. The results clearly suggest that after the THF:MCH composition reaches 40:60, the aggregation begin to occur (Figure S4). Similar trend was observed upon addition of H_2O in THF as shown in Figure 3b. At the 30:70 (THF:H_2O) solvent composition the decrease in UV-Vis absorption peak intensities at 344 nm, 360 nm and 380 nm was observed and at 10:90 (THF: H_2O) solvent composition significant changes was noted. The decrease in absorption peak intensities with an increase in % of MCH (Figure 3a) and H_2O (Figure 3b) in THF clearly indicating the aggregation of **NDI-Trp-GLU** takes place *via* π-π interaction of NDI core along with H-bonding of peptide amide units.

The fluorescence emission spectra of **NDI-Trp-GLU**exhibits two strong emission peaks at 410 nm and 432 nm (λ_{ex}= 380 nm) as shown in Figure 3c and Figure 3d. A solvent dependent emission spectroscopic study of **NDI-Trp-GLU** was performed to get detail insight of aggregation state. At first we performed titration of **NDI-Trp-GLU** in THF solution by varying the concentration of MCH (Figure 3c). Upon increasing MCH%, the emission peak intensities decreased and were steady after 90% of MCH. These results, similar to H-aggregate state quenching of emission spectra, occurs due to rapid inter-band relaxation[20]. Similar emission quenching of **NDI-Trp-GLU** was observed in THF solution with increasing % of H_2O keeping the fixed dye concentration (Figure 3d). Upon increase in the H_2O percentage (>90%) the fluorescence emission spectral peak intensities significantly decreased. These results indicate the **NDI-Trp-GLU** undergoes self-aggregation.

Scanning electron microscopy studies

Furthermore, Field Emission Scanning Electron Microscopy (FE-SEM) were studied to gain detail insight into the self-assembled morphology of the **NDI-Trp-GLU** (Figure 4). The drop-cast method was used to prepare the sample onto a silicon wafer substrate and various microstructures of the **NDI-Trp-GLU**was observed after evaporation of the solvent. Firstly, the self-assembly was carried out in THF: MCH = 40:60 vol% and 20:80 vol% solvent compositions. The self-assembly of **NDI-Trp-GLU** in THF: MCH (40:60, vol%) results in a microsheet like morphology with several micrometers in length (Figure 4a and Figure 4b). It is observed that the microsheet puzzle piece does not fit pair wise with any neighbouring structures. Such geometrically frustrated self-assembled morphologies are less understood than the standard morphologies[21]. Furthermore, at higher fraction of MCH in THF: MCH (20:80, vol%) solvent composition **NDI-Trp-GLU** exhibit fibril networks (Figure 4c and Figure 4d). The observed fibres are of several micrometers length with 50-80 nm in diameter. Thus, self-assembled structures obtained from THF in presence of 60 vol% and 80 vol% MCH implies that the presence of MCH content *i.e.* polarity of solvent is responsible for formation of particular morphologies such as geometrically frustrated puzzle and fibril networks. We presume that molecular aggregation of **NDI-Trp-GLU** take place *via* non-covalent interactions such as amide hydrogen bonding and π-π stacking of intermolecular NDI core as well as indole ring of tryptophan segment. The solubility of **NDI-Trp-GLU** in THF: MCH (20:80, vol%) are poorer than that at lower fraction of MCH = 60 vol%. At higher fraction of MCH interaction between **NDI-Trp-GLU** and solvent is weaker and intermolecular interaction between NDI cores is relatively stronger results into microsheets during the aggregation.

We also investigated supramolecular self-assembly of **NDI-Trp-GLU** in THF:H_2O = 40:60 vol% and 20:80 vol% solvent mixtures by means of SEM imaging. The interactions between the **NDI-Trp-GLU** molecule and mixed solvent can be controlled by adjusting water volume in THF. SEM images of **NDI-Trp-GLU** with THF:H_2O = 40:60 vol% ratios on silicon wafer substrate exhibited nanoflower assembly with a diameter of ~500-800 nm (Figure 5a and Figure 5b). The self-assembly of **NDI-Trp-GLU** in THF:H_2O mixture the f_w increases to 80 vol% yields several micrometer long thick fibril network with a 50-80 nm width (Figure 5c and Figure 5d). The solubility of **NDI-Trp-GLU** in THF:H_2O solvent

compositions. The aggregate formation is initiated by the presence of water fractions in THF. The driving force for aggregation is the mutual interaction between NDI molecules *via* non-covalent interactions such as amide hydrogen bonding and π-π stacking effects. **NDI-Trp-GLU** molecule consists of non-polar subunits such as rigid NDI aromatic core and glutamate. Increase in f_w causes attractive interaction between NDI core and repulsive interaction between aromatic NDI core and polar solvent, resulting into different type of self-assembled aggregates in the THF:H_2O = 20:80 vol% solvent mixtures (Figure 5c and Figure 5d).

Dynamic light scattering studies

Dynamic light scattering (DLS) method was employed to investigate the self-assembly of **NDI-TRP-GLU** in THF:MCH (40:60 and 20:80, *v/v*) (Figure S5a) and THF:H_2O (40:60 and 20:80, *v/v*) (Figure S5b) solvent compositions. It was observed that in THF:MCH (40:60*v/v*), **NDI-Trp-GLU** yields 88% of assemblies with an average diameter of 479.6 nm. However, in THF:MCH (20:80*v/v*), the hydrodynamic diameter of **NDI-Trp-GLU** assemblies increased to 1693 nm (86.2%). Furthermore, in presence of more polar solvent such as THF:H_2O (40:60*v/v*) the hydrodynamic diameters of assemblies was 343.7 nm with 100% intensity., where as with increased water content *i.e*. THF:H_2O (20:80, *v/v*) solvent compositions the average diameter of assemblies was found to be 2922 nm with 100% intensity. These findings suggest that change in solvent polarity causes repulsive interactions between aromatic NDI and more polar solvent mixes may play

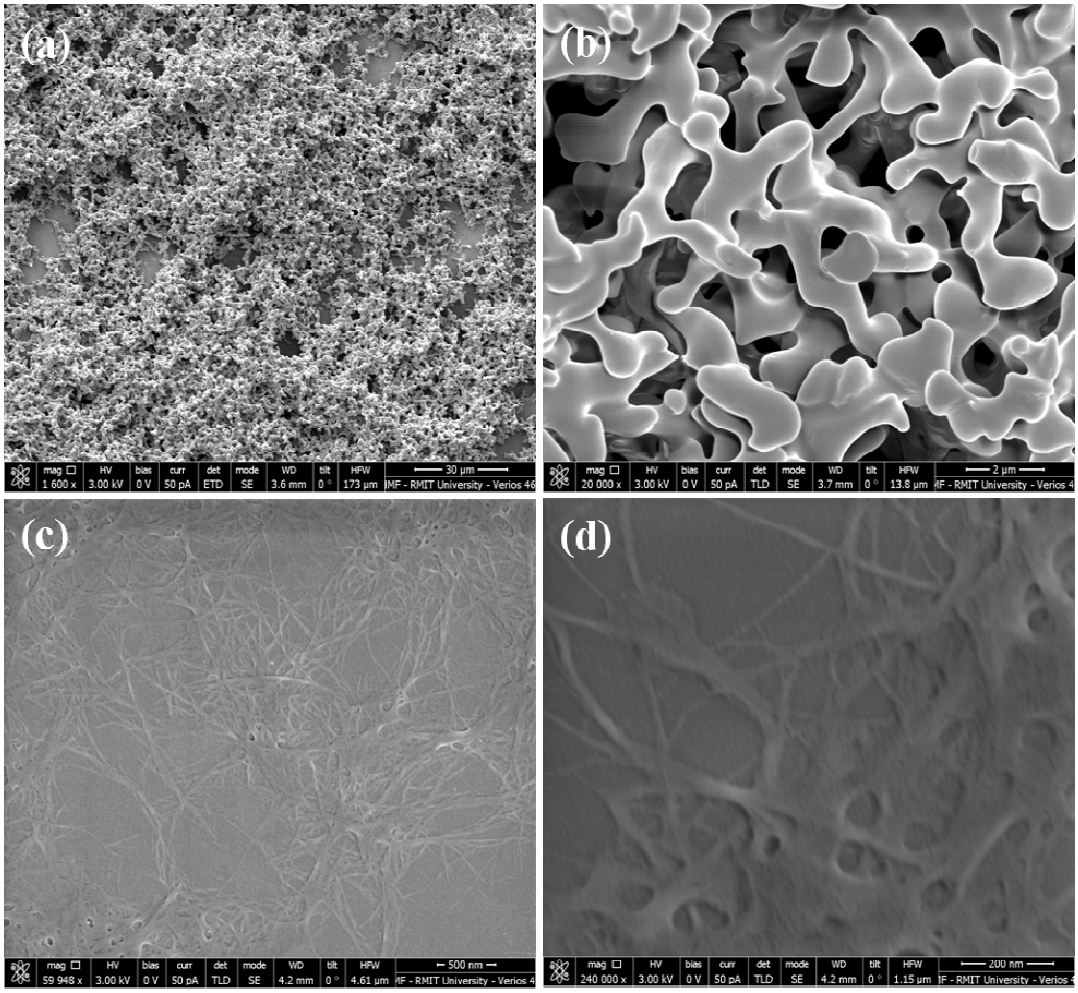

Figure 4 — SEM images of the aggregation morphologies of **NDI-Trp-GLU** in THF upon addition of (a) & (b) 60% MCH; (c) & (d) 80% MCH at RT.

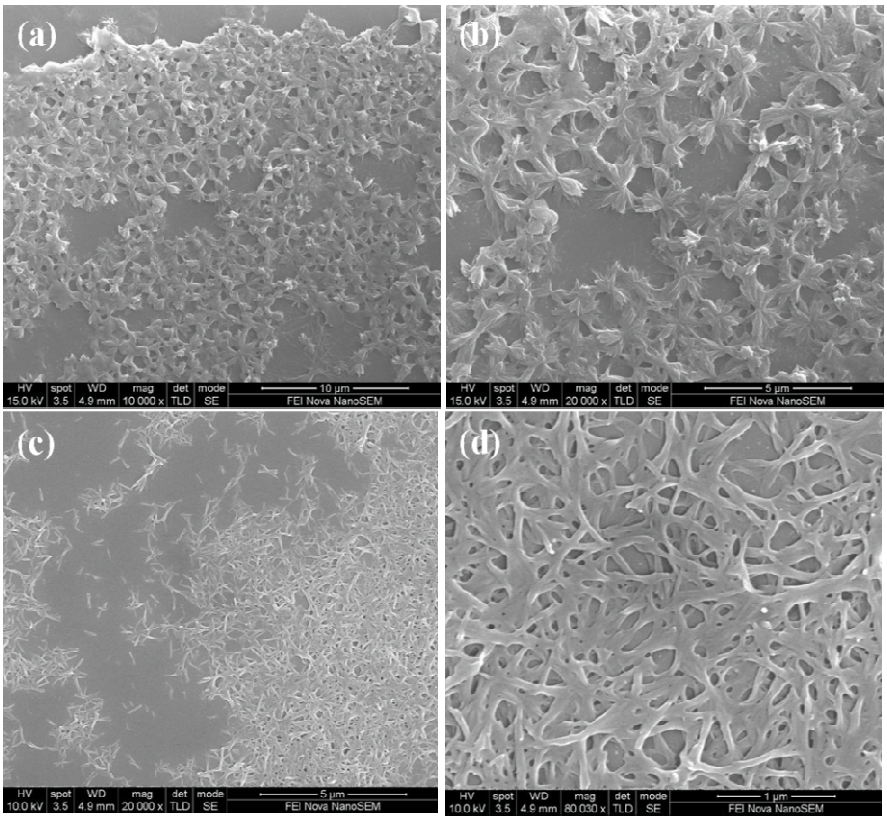

Figure 5 — SEM images of the aggregation morphologies of **NDI-TRP-GLU** in THF upon addition of (a) & (b) 60% H_2O; (c) & (d) 80% H_2O at RT.

an important role in controlling the assembly formation.

FT-IR Study

To understand the self-assembly mechanism, FT-IR was employed to record the IR spectra of **NDI-Trp-GLU**. IR spectra of **NDI-Trp-GLU** were investigated at various solvent compositions such as THF:H_2O (40:60 and 20:80, *v/v*)as shown in Figure 6 and THF:MCH (40:60 and 20:80, *v/v*) shown in SI (Figure S6). In THF **NDI-Trp-GLU** exhibited vibrational stretching frequencies at 1669 cm^{-1} (imide), 1707 cm^{-1} (amide) and 1738 cm^{-1} (carboxylate) for three carbonyl functional subunits. Upon incremental addition of water in THF solution of **NDI-Trp-GLU** such as THF:H_2O (40:60 and 20:80, *v/v*), it was observed that the amide and carboxylate carbonyl peak disappeared dramatically. The disappearance of peaks at 1707 cm^{-1} (amide) and 1738 cm^{-1} (carboxylate) are attributed to the involvement of carbonyl group in intermolecular hydrogen bond formation during assembly process. The imide carbonyl stretching frequency peak at 1669

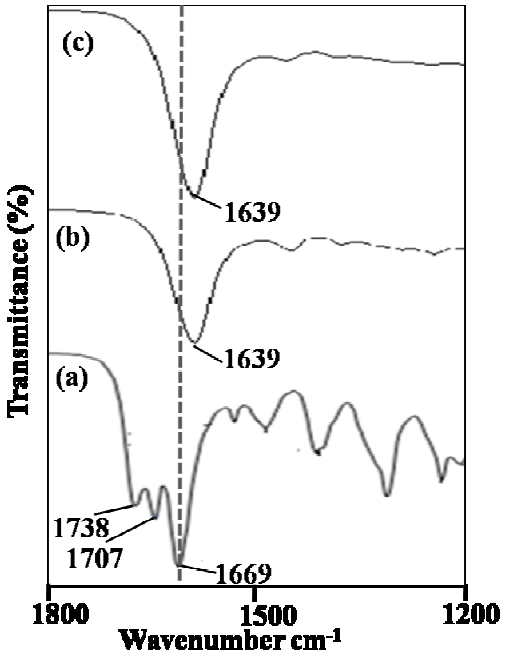

Figure 6 — FT-IR spectra (carbonyl region) of **NDI-Trp-GLU** in (a) THF and THF:H_2O (b)40:60% and (c) 20:80%, respectively.

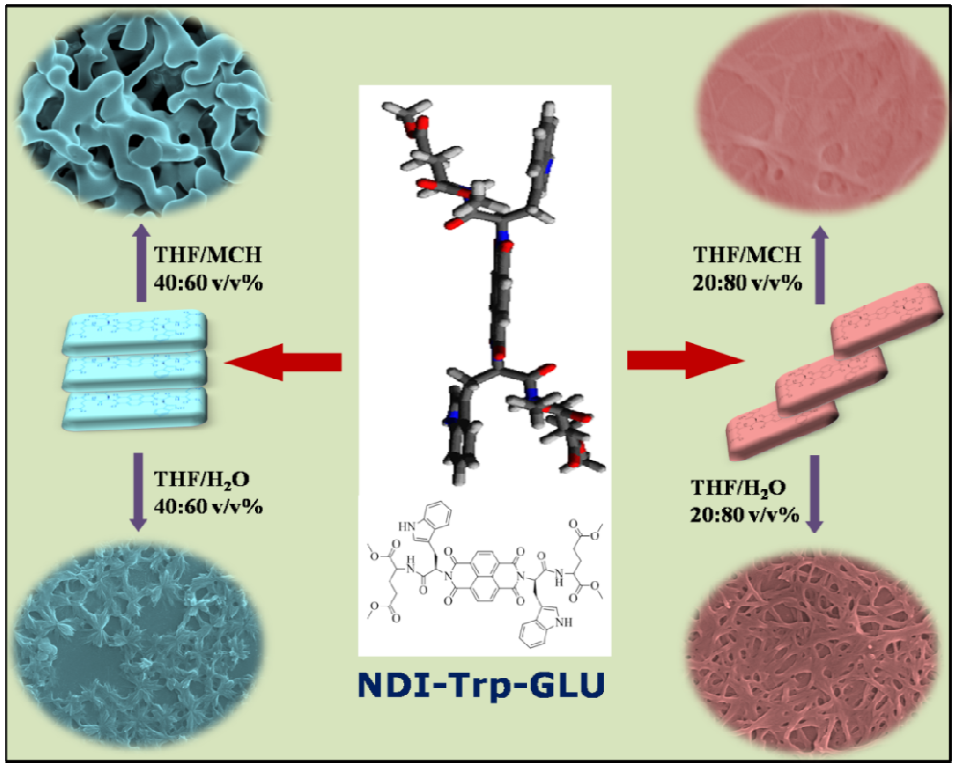

Figure 7 — Schematic representation of assembly formation

cm^{-1} showed small shift to 1639 cm^{-1}. Similar trend was observed *i.e.* peaks at 1707 cm^{-1} (amide) and 1738 cm^{-1} (carboxylate) with the addition of MCH (60% and 80% vol) to the THF solution of **NDI-Trp-GLU** (Figure S6). For THF:MCH (40:60 and 20:80, *v/v*) solvent composition the imide carbonyl peak at 1669 cm^{-1} shifts to 1670 cm^{-1} and 1680 cm^{-1}. These result suggests that the aggregation mode of **NDI-Trp-GLU** in THF:H_2O and THF:MCH are not equivalent and it depends on polarity of solvents and their percentage in THF.

Mechanism of assembly formation

The formed nano- to micro-structures of **NDI-Trp-GLU** indicates intermolecular π-π stacking interactions of the NDI cores, as well as H-bonding interaction between the carboxylic acid give directional growth. Figure 7 is a schematic representation of the aggregation mode of **NDI-Trp-GLU** in the self-assembled state, giving a supramolecular thick microfibers network, along with microflowers through increasing proportion of MCH and H_2O in THF solvent, respectively, which depends on the balance between the hydrophobic π-π interactions and H-bonding interaction. This clearly suggests that solvophobic control is important for self-assembly phenomenon in which NDI core moieties lead to in plane intermolecular interaction while the peptide moieties on both the side of imide helps the stacking of the molecules *via* H-bonding.

Conclusions

Herein, we demonstrated for the first time synthesis of NDI bearing tryptophan along with L-glutamic acid ester (**NDI-Trp-GLU**) and their self-assembly in THF:MCH and THF:water with varying proportion of MCH and water, respectively. **NDI-Trp-GLU** self-assembled into microsheets like supramolecular structures in 60% MCH, long fibrils in 80% MCH, however, in polar solvent such as water in THF flower like structures was observed. These results clearly demonstrate that one can easily control morphology by controlling polar and non-polar solvent mixture.

Supplementary Information

Supplementary information is available in the journal website

Acknowledgments

SVB (IICT) is thankful to SERB (SB/S1/IC-009/2014), New Delhi, India for financial support and IICT

Commun. No. IICT/Pubs./2018/132. SPG acknowledges the UGC for financial support under SRF. RSB is grateful for financial support from CSIR, New Delhi, under the SRA scheme [(13(8772)-A/2015-Pool]. SVB (GU) acknowledges to UGC for financial support under UGC-FRP programme and professorship. ALP acknowledges use of Gaussian 09 procured under the DST-FIST Scheme (Sanction No. FS/FST/PSI-018/2009).

Competing financial interests

The authors declare no competing interests.

References

1 Hoeben F J M, Jonkheijm P, Meijer E W & Schenning A P H J, *Chem Rev*, 105 (2005) 1491; (b) Lehn J M, *Angew Chem Int Ed*, 52 (2013) 2836; (c) Babu S S, Praveen V K & Ajayaghosh A, *Chem Rev*, 114 (2014) 1973; (d) Mahadevi A S & Sastry G N, *Chem Rev*, 116 (2016) 2775.

2 (a) Ogi S, Sugiyasu K, Manna S, Samitsu S & Takeuchi M, *Nat Chem*, 6 (2014) 188; (b) Jain A & George S J, *Mater Today*, 18 (2015) 206; (c) Wang H, Feng Z & Xu B, *Chem Soc Rev*, 46 (2017) 2421; (d) Bai Y, Luo Q & Liu J, *Chem Soc Rev*, 45 (2016) 2756.

3 Kobaisi M A, Bhosale S V, Latham K, Raynor A M & Bhosale S V, *Chem Rev*, 116 (2016) 11685.

4 (a) Shao J, Chang J & Chi C, *Chem Asian J*, 9 (2014) 253; (b) Zhan X, Facchetti A, Barlow S, Marks T J, Ratner M A, Wasielewski M R & Marder S R, *Adv Mater*, 23 (2011) 268; (c) Weil T, Vosch T, Hofens J, Peneva K & Mullen K, *Angew Chem Int Ed*, 49 (2010) 9068; (d) Srivani D, Gupta A, Bhosale S V, Puyad A L, Xiang W, Li J, Evans R A & Bhosale S V, *Chem Commun*, 53 (2017) 7080; (e) Srivani D, Agarwal A, Bhosale S V, Puyad A L, Xiang W, Evans R A, Gupta A & Bhosale S V, *Chem Commun*, 53 (2017) 11157; (f) Ma L, Guo S, Sun J, Zhang C, Zhao J & Guo H, *Dalton Trans*, 42 (2013) 6478; (g) Hu B-L, Zhang K, An C, Pisula W & Baumgarten M, *Org Lett*, 19 (2017) 6300.

5 (a) Ren G, Ahmed E & Jenekhe S A, *J Mater Chem*, 22 (2012) 24373; (b) Choudhury P, Das K & Das P K, *Langmuir*, 33 (2017) 4500; (c) Nandre K P, Bhosale S V, Krishna K R, Gupta A & Bhosale S V, *Chem Commun*, 49 (2013) 5444.

6 (a) Molla M R, Gehrig D, Roy L, Kamm V, Paul A, Laquai F & Ghosh S, *Chem Eur J*, 20 (2014) 760; (b) Das A & Ghosh S, *Angew Chem Int Ed*, 53 (2014) 1092; (c) Billeci F, D'Anna F, Chiarotto I, Feroci M & Marullo S, *New J Chem*, 41 (2017) 13889.

7 (a) Hosseinkhani H, Hong P-D & Yu D-S, *Chem Rev*, 113 (2013) 4837; (b) Wang J, Liu K, Xing R & Yan X, *Chem Soc Rev*, 45 (2016) 5589; (c) Edwards-Gayle C J C & Hamley I W, *Org Biomol Chem*, 15 (2017) 5867.

8 Babar D G & Sarkar S, *Appl Nanosci*, 7 (2017) 101.

9 Padnya P L, Khripunova I A, Mostovaya O A, Mukhametzyanov T A, Evtugyn V G, Vorobev V V, Osin Y N & Stoikov I I, *Beilstein J Nanotechnol*, 8 (2017) 1825.

10 Chakraborty G, Chowdhury M P & Saha S K, *Langmuir*, 33 (2017) 6581.

11 Zhang C, Gao P & Liu M, *Chem Commun*, 2005, 462.

12 (a) Ponnuswamy N, Dan Pantoş G, Smulders M M J & Sanders J K M, *J Am Chem Soc*, 134 (2012) 566; (b) Das A & Ghosh S, *Chem Commun*, 52 (2016) 6860.

13 Tu S S, Kim H, Joseph J, Modarelli D A & Parquette J R, *J* AM CHEM SOC, 133 (2011) 19125.

14 Goskulwad S P, La D D, Bhosale R S, Al Kobaisi M, Bhosale S V & Bhosale S V, *RSC Adv*, 6 (2016) 39392.

15 Goskulwad S P, La D D, Bhosale R S, Al Kobaisi M, Jones L A, Bhosale S V & Bhosale S V, *ChemistrySelect*, 3 (2018) 1460.

16 (a) Avinash M B & Govindaraju T, *Nanoscale*, 3 (2011) 2536; (b) Hu Z, Arrowsmith R L, Tyson J A, Mirabello V, Ge H, Eggleston I M, Botchway S W, Dan Pantos G & Pascu S I, *Chem Commun*, 51 (2015) 6901.

17 Gaussian 09, Revision C.01, Frisch M J, *et al.* (2009) Gaussian Inc., Wallingford CT (2009).

18 Avogadro: an open-source molecular builder and visualization tool, Version 1.1.0. http://avogadro.openmolecules.net/.

19 Hanwell M D, Curtis D E, Lonie D C, Vandermeersch T, Zurek E & Hutchison G R, *J Cheminform*, 4 (2012) 1.

20 Rösch U, Yao S, Wortmann R & Würthner F, *Angew Chem Int Ed*, 45 (2006) 7026.

21 Lenz M & Witten T M, *Nat Phys*, 13 (2017) 1100.